

Monoclonal Antibody to Vascular Endothelial-cadherin Is a Potent Inhibitor of Angiogenesis, Tumor Growth, and Metastasis¹

Fang Liao, Yiwen Li, William O'Connor, Lucia Zanetta, Rajiv Bassi, Angel Santiago, Jay Overholser, Andrea Hooper, Paolo Mignatti, Elisabetta Dejana, Daniel J. Hicklin,² and Peter Bohlen

Departments of Immunology and Molecular and Cell Biology and Research, ImClone Systems Incorporated, New York, New York 10014 [F. L., Y. L., W. O., R. B., A. S., J. O., A. H., D. J. H., P. B.]; Istituto di Ricerche Farmacologiche, Mario Negri, 20157 Milan, Italy [L. Z., E. D.]; and Departments of Surgery and Cell Biology, New York University School of Medicine, New York, New York 10016 [P. M.]

Abstract

Vascular endothelial-cadherin (VE-cad) is an endothelial cell-specific adhesion molecule that is crucial for proper assembly of vascular tubes. Here we show that a monoclonal antibody (BV13) directed to the extracellular region of VE-cad inhibits formation of adherens junctions and capillary-like structures by endothelial cells and blocks angiogenesis in the mouse cornea and in Matrigel plugs *in vivo*. Systemic administration of BV13 markedly decreases the growth of s.c. Lewis lung or human A431 epidermoid tumors and strongly suppresses the growth of Lewis lung metastases. These data demonstrate that VE-cad is essential for postnatal angiogenesis and thus validate VE-cad as a novel target for antiangiogenesis agents.

Introduction

Angiogenesis, the formation of capillaries from preexisting blood vessels, occurs in a variety of physiological and pathological settings, the most relevant of which are tumor growth and metastasis (1). Angiogenesis inhibitors are recognized as potentially useful agents for treating angiogenesis-associated diseases, *e.g.*, cancer. Although a large number of angiogenesis inhibitors have been reported, only a few appear to target endothelial cells or molecules important for angiogenesis. VEGF³ and its receptors (Flk-1/KDR and Flt-1) represent promising and well-studied targets for antiangiogenesis agents because of the highly specific action of VEGF on endothelial cells and the importance of VEGF receptors on activated endothelium in mediating angiogenic signals (2, 3). Other inhibitors have been described that target certain adhesion molecules (*e.g.*, $\alpha_v\beta_3$ and $\alpha_v\beta_5$ integrins; Ref. 4) or pericellular protease activation systems (plasminogen activator receptor; Ref. 5) associated with the vasculature. Many angiogenesis inhibitors are directed against less specific (*e.g.*, metalloproteinase inhibitors; Ref. 6) or as yet undefined targets (*e.g.*, angiostatin and endostatin; Refs. 7 and 8). It would appear, however, that the complex nature of the angiogenic process and its regulation should provide an abundant source of additional molecular targets.

Our recent studies (9, 10) aimed at developing angiogenesis inhibitors that target the VE-cad, an endothelial cell-specific cadherin localized at specialized cell-cell contact regions referred to as adherens junctions. Accumulating evidence implicates VE-cad in various aspects of vascular biology related to angiogenesis, including endo-

thelial cell migration (9) and survival (11), contact-induced growth inhibition (12), vascular integrity (13), and, most notably, endothelial cell assembly into tubular structures (14). VE-cad-null mouse embryos exhibit severely impaired assembly of vascular structures, which results in embryonic lethality at day 9.5 (11), implicating VE-cad as an important mediator in developmental angiogenesis. VE-cad represents one of the most endothelial cell-specific molecules. Its restricted distribution and unique biological function distinguish VE-cad as a potential target for endothelial cell-specific events, *e.g.*, angiogenesis.

Materials and Methods

Cells and Media. Mouse Lewis lung carcinoma cells (clone D122-96; from Dr. L. Eisenbach; Weizmann Institute of Science, Rehovot, Israel), human A431 epidermoid carcinoma cells (American Type Culture Collection, Manassas, VA; ATCC CRL-1555), and mouse endothelioma cells (bEND.3; from Dr. T. N. Sato; University of Texas Southwestern Medical Center, Dallas, TX; Ref. 15) were grown in DMEM (Life Technologies, Inc., Gaithersburg, MD) containing 10% fetal bovine serum (HyClone Laboratories, Logan, UT). Mouse endothelial cells (1G11; Ref. 16) were grown in DMEM containing 20% fetal bovine serum supplemented with 100 $\mu\text{g/ml}$ endothelial cell growth supplement (Sigma, St. Louis, MO) and 100 $\mu\text{g/ml}$ heparin (Sigma).

Anti-VE-cad Antibody. The rat anti-VE-cad monoclonal antibody BV13 was developed and characterized as described previously (13). The antibody was purified from conditioned medium by protein G-Sepharose chromatography. All antibody preparations used for animal studies, including control rat IgG (Jackson ImmunoResearch Laboratories, West Grove, PA), contained ≤ 1.25 endotoxin units/ml endotoxin as assessed by the *Limulus* Amebocyte Lysate assay kit (BioWhittaker, Walkersville, MD).

In Vitro Angiogenesis Assays. Capillary tube formation of 1G11 cells was performed in collagen sandwich gels as described previously (17). In brief, type I collagen from rat tail was diluted to a concentration of 1 mg/ml, and the pH was neutralized by adding 0.1 volume of 10 \times MEM (Life Technologies). Aliquots of collagen (250 μl) were added to each well of 24-well plates and incubated at 37°C until solidified. 1G11 cells were then seeded onto collagen-coated wells, and cell monolayers were established by incubation for 24 h at 37°C. Unattached cells were then aspirated, and overlying collagen gels were generated using the same procedure as described above. For the tube assay performed in the Matrigel system with bEND.3 cells, 2 \times 10⁴ cells were plated onto each well of a 24-well plate coated with a layer of Matrigel (BD Biosciences, Bedford, MA) and cultured for 24 h in MCDB133 medium (Life Technologies, Inc.). Antibody BV13 was added to the collagen/Matrigel gels and culture media, and the inhibitory effect on tube formation was assessed under a Zeiss microscope.

In Vivo Angiogenesis Assays. The mouse corneal micropocket assay was performed as described previously (18) using hydon-coated sucralfate pellets containing 50 ng of bFGF (R&D Systems, Minneapolis, MN) or 200 ng of VEGF₁₆₅ with or without the addition of BV13 (1 μg). For systemic treatment, 50 μg of BV13 were administered to mice *i.p.* twice weekly starting 24 h after pellet implantation. Alginate tumor cell encapsulation and Matrigel plug assays were performed as described previously (19). In both assays, the antibodies were administered *i.p.* twice weekly at 25 or 50 $\mu\text{g/dose}$, and angiogenesis was

Received 8/21/00; accepted 10/31/00.

The costs of publication of this article were defrayed in part by the payment of page charges. This article must therefore be hereby marked *advertisement* in accordance with 18 U.S.C. Section 1734 solely to indicate this fact.

¹ Supported in part by a NIH Small Business Innovation and Research grant.

² To whom requests for reprints should be addressed, at Department of Immunology, ImClone Systems Incorporated, 180 Varick Street, New York, NY 10014. Phone: (646) 638-5035; Fax: (212) 645-2054; E-mail: danh@imclone.com.

³ The abbreviations used are: VEGF, vascular endothelial growth factor; Flk-1/KDR, fetal liver kinase 1/kinase insert domain containing receptor; Flt-1, FMS-like tyrosine kinase 1; VE-cad, vascular endothelial-cadherin; bFGF, basic fibroblast growth factor; PECAM, platelet/endothelial cell adhesion molecule.

quantitated by measuring the uptake of FITC-dextran into plugs or beads. The Matrigel plugs were removed 21 days after implantation, quantitated, and processed for histological examination as described previously (19).

Mouse Tumor Models. Lewis lung tumors were established by injecting 2×10^6 D122 tumor cells s.c. into the right flank of C57BL/6 mice. Twenty-four h later, mice received twice weekly i.p. injections of various doses of BV13 or control IgG. Tumors were measured twice weekly with calipers, and tumor volumes were calculated using the formula $[\pi/6 (w_1 \times w_2 \times w_2)]$, where w_1 represents the largest tumor diameter, and w_2 represents the smallest tumor diameter. For the pulmonary metastasis model, mice received an intrafootpad injection of 1×10^5 D122-96 tumor cells (19). When footpad tumors reached 5 mm in diameter, the tumor-bearing leg was surgically ligated. Mice were then divided into three groups receiving i.p. injections of either BV13 (25 and 50 $\mu\text{g}/\text{dose}$) or control IgG (50 $\mu\text{g}/\text{dose}$) twice weekly for 3 weeks. Mice were then sacrificed, and the lungs were removed and weighed to measure the metastatic load, and tumor nodules on the lung surface were also counted as described previously (19).

Human Tumor Xenograft Model. The s.c. human epidermoid (A431) tumors were established by injecting 2×10^6 tumor cells mixed in an equal volume of Matrigel into athymic nude mice s.c. in the right flank. Tumors were allowed to reach 150–200 mm^3 in size, and then randomized groups of 10 animals received twice-weekly i.p. injections of BV13 or control IgG (50 $\mu\text{g}/\text{dose}$). Tumors were measured twice weekly with calipers, and tumor volumes were calculated as described above.

Histology. Six- μm sections of Matrigel plugs were stained with anti-von Willebrand factor antibody (DAKO Corp., Carpinteria, CA) as described previously (19). A431 tumors or lungs from mice bearing lung metastases were fixed in 10% neutral buffered formalin overnight at 4°C, embedded in paraffin or frozen with OCT and sectioned. All paraffin-embedded tissue sections were stained with Mayer's H&E (Sigma). Anti-PECAM staining or terminal deoxynucleotidyl transferase-mediated nick end labeling was performed as described previously (19) using *In Situ* Cell Death Detection Kit (Boehringer Mannheim, Indianapolis, IN). Light and fluorescent images of immunostained tissues were digitized with a Sony camera and Scion CG-7 framegrabber and captured with NIH Image Software.

Statistical Analysis. Vessel density counts, tumor volume, and lung metastasis were analyzed using the Student's *t* test. Analyses were computed using the statistical package in SigmaStat version 4.0 (Jandel Scientific, San Rafael, CA).

Results

Monoclonal Antibody to VE-cad Inhibits Angiogenesis *in Vitro* and *in Vivo*. The role of VE-cad in postnatal angiogenesis and, in particular, in tumor angiogenesis has not been addressed in previous studies. We hypothesized that blocking VE-cad-mediated homophilic interaction between endothelial cells would inhibit neo-

vascularization. To test this hypothesis, we used a rat monoclonal antibody (BV13; Ref. 13) directed against the extracellular region of mouse VE-cad. We first addressed the question of whether BV13 can block the formation of endothelial cell adherens junctions in an *in vitro* angiogenesis assay using mouse primary endothelial cells (1G11; Ref. 16) and the mouse endothelioma cell line bEND.3 (15) seeded on collagen and Matrigel gels, respectively. These two cell lines express a comparable level of VE-cad and form stable adherens junctions as evidenced by the junctional VE-cad staining pattern and intercellular permeability (data not shown). At concentrations as low as 5 $\mu\text{g}/\text{ml}$, BV13 completely blocked the formation of 1G11 and bEND.3 tubular structures, whereas a control antibody (rat IgG1) had no effect (data not shown). Apoptosis of 1G11 or bEND.3 cells was not observed in response to BV13 antibody treatment in the tube assays. These results are similar to those reported previously with anti-human VE-cad antibodies on human umbilical vein endothelial cells (14, 17) and suggest that BV13 interferes with VE-cad-mediated contact between adjacent endothelial cells, thereby blocking the formation of adherens junctions and the assembly of vascular tubes.

To evaluate whether blocking VE-cad homophilic binding could inhibit angiogenesis *in vivo*, we tested the effect of BV13 on angiogenesis in three mouse models. In the mouse corneal micropocket assay (18), hydron pellets containing 50 ng of bFGF and 1 μg of an irrelevant antibody (rat IgG1) induced a marked neovascularization derived from the limbic vessels (Fig. 1a, left panel). In contrast, the eyes of animals receiving BV13-containing pellets (1 $\mu\text{g}/\text{pellet}$) showed much fewer and thinner corneal capillaries (Fig. 1a, right panel) with a resulting 72% decrease in the vascular area (Fig. 1b). Similar results were obtained when BV13 was administered locally in hydron pellets containing 200 ng of VEGF₁₆₅ or systemically (50 μg BV13/mouse, twice weekly) in mice receiving implants with pellets containing 50 ng of bFGF. VEGF-stimulated corneal angiogenesis was inhibited by 65% with locally administered antibody, whereas bFGF-induced corneal angiogenesis was inhibited by 47% with systemic antibody administration (data not shown). To confirm the antiangiogenic effect of BV13, we also tested this antibody in the Matrigel plug assay (19). In this assay, extensive angiogenesis was induced by s.c. injection of Matrigel supplemented with bFGF (500 ng) and VEGF₁₆₅ (10 μg). In contrast, plugs without growth factors were virtually devoid of vessels. Two doses of BV13 (25 and 50 $\mu\text{g}/\text{dose}$) were chosen based on dose-response studies and the results

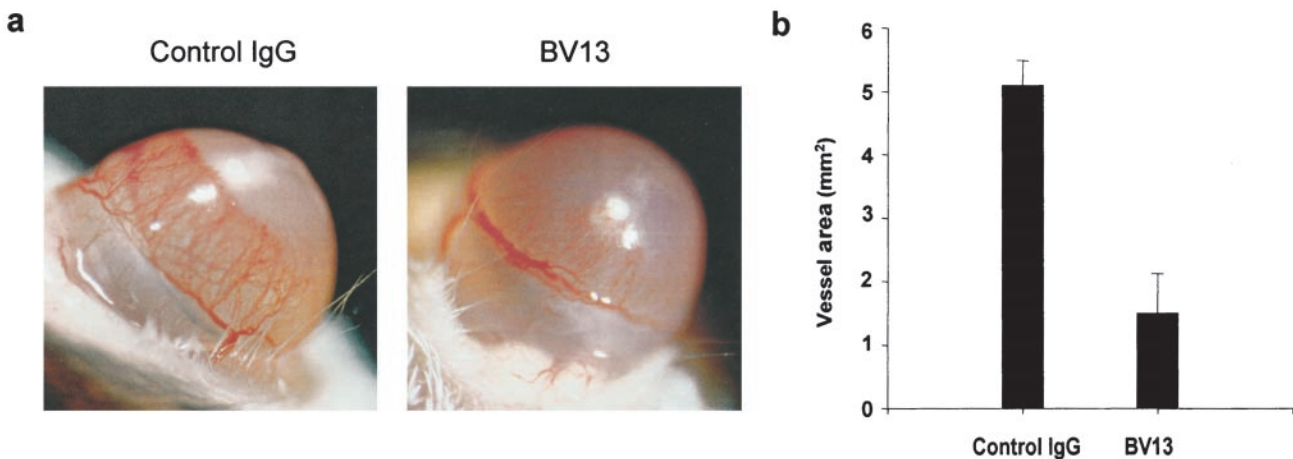


Fig. 1. Antibody BV13 inhibits angiogenesis in mouse cornea. *a*, eyes of mice photographed 6 days after implantation of hydron pellets containing 50 ng of bFGF and 1 μg of either BV13 or control IgG. *b*, vascular areas of corneal angiogenesis in mice that received hydron pellets containing 50 ng of bFGF and 1 μg of either BV13 or control IgG. Mean \pm SE ($n = 6$) values from a representative experiment are shown.

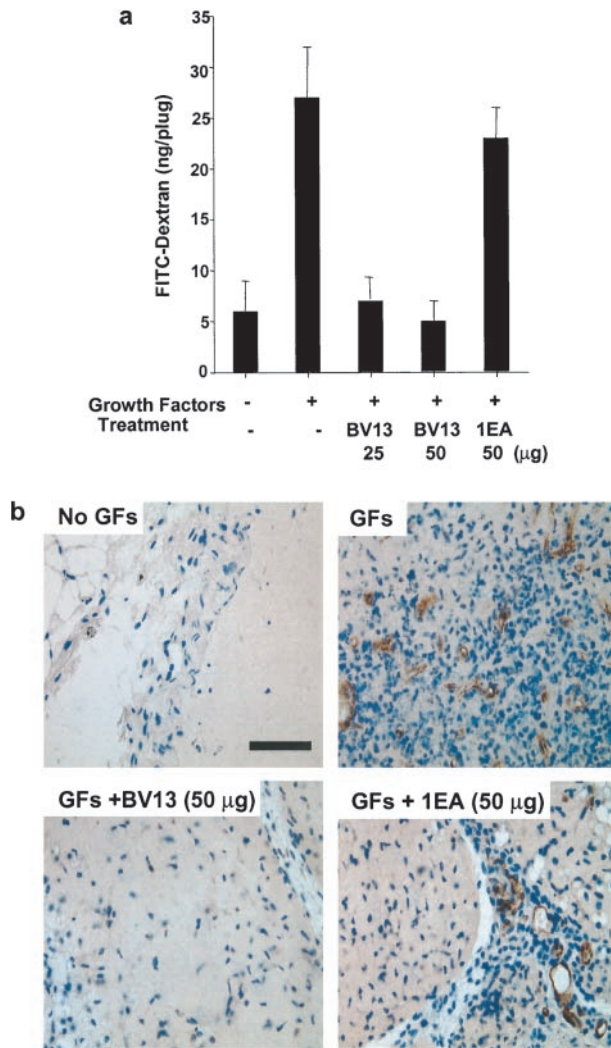


Fig. 2. Antibody BV13 inhibits angiogenesis in a Matrigel plug assay. *a*, Matrigel plug vascularization was quantitated by FITC-dextran uptake as described previously (19), and data are presented as the mean \pm SE ($n = 12$). *b*, immunohistochemical staining of plug sections with anti-von Willebrand factor antibody shows reduced numbers of endothelial cells and vessel structures (brown staining) in BV13-treated plugs. Scale bar, 100 μ m.

of previous studies (13). BV13 was administered to mice by i.p. injection twice weekly for 21 days. Pharmacokinetic studies were performed to determine a serum half-life of BV13 antibody in mice of approximately 48 h.⁴ Treatment with either dose of BV13 resulted in a >90% reduction of cellularity and microvessel density in growth factor-supplemented plugs as compared with control antibody (Fig. 2). Similar results were obtained using an Alginate tumor cell encapsulation model (Ref. 19; data not shown). These results demonstrate that BV13 has potent antiangiogenic activity *in vivo*.

Antibody BV13 Inhibits Tumor Growth. To assess whether blocking VE-cad homophilic binding could inhibit tumor angiogenesis and subsequent growth of tumors, we tested the effect of BV13 treatment in the Lewis lung carcinoma and human A431 epidermoid carcinoma models (19). In the Lewis lung tumor model, s.c. tumors grew rapidly in the untreated or control IgG-treated animals and reached a size of >1500 mm³ by day 24, after which the mice became moribund, and the experiments were terminated. In contrast, tumors in BV13-treated mice grew much more slowly. A dose-dependent effect on tumor growth was observed with 50 μ g of BV13 resulting in

significant tumor inhibition (65% and 20% inhibition with 50 and 25 μ g of BV13, respectively; $P < 0.05$; Fig. 3*a*). In the A431 s.c. human tumor xenograft model, tumor-bearing mice were treated i.p. with 50 μ g of BV13 or control IgG twice weekly. BV13 significantly inhibited A431 tumor growth relative to control antibody (75%; $P < 0.05$; Fig. 3*b*). Doses of BV13 lower than 50 μ g had no significant effect on the growth of A431 tumors compared with control antibody. Histological examination of tumors removed from animals after antibody treatment for various periods of time (*i.e.*, 2, 4, and 6 weeks) showed dramatic differences between BV13- and control IgG-treated groups. Tumors from animals receiving BV13 treatment for 2 weeks showed enhanced tumor necrosis and markedly decreased vessel density (>80%; $P < 0.05$; Fig. 3*c*) as compared with control IgG-treated mice. Double staining of tumors with anti-PECAM antibody and terminal deoxynucleotidyl transferase-mediated nick end labeling demonstrated endothelial cell apoptosis in the vasculature of the BV13-treated A431 tumors (Fig. 3*c*) as well as increased tumor cell apoptosis. Analysis of sections at 4 or 6 weeks of BV13 treatment did not show a significant difference in endothelial cell or tumor cell apoptosis from that observed at 2 weeks. Interestingly, BV13-induced apoptosis was prominent only in the tumor tissues, whereas similar treatment resulted in no observable apoptosis in normal tissues such as lungs, hearts, and kidneys (data not shown). This finding suggests that tumor vasculature is more susceptible to BV13 treatment.

Antibody BV13 Inhibits Tumor Metastasis. To examine whether BV13 could inhibit the growth of tumor metastases, the antibody was tested in a Lewis lung metastasis model. Primary Lewis lung tumors were established in the footpads of mice and then removed when they reached 5 mm in size (3–4 weeks), at which time pulmonary metastases had developed. Treatment with BV13 was initiated 24 h after removal of the primary tumor and continued for the duration of the experiment. All control antibody-treated mice had large numbers of surface lung metastases by 60 days. Growth of pulmonary metastases was significantly inhibited by BV13 treatment as evidenced by reduced lung weight (>80%) and the decreased number of lung metastases (> 90%) compared with the control group (Fig. 4*a*). Histological examination showed that pulmonary metastasis was rarely detected as small nests of tumor cells in the lungs of mice treated with 25 μ g of BV13 (Fig. 4*b*). Several mice (7 of 10) treated with 50 μ g of BV13 had no evidence of micrometastases. These results suggest that in addition to affecting the growth of a primary tumor, BV13 also inhibits the growth of metastases. It is noteworthy that BV13 treatment affected the formation of metastases much more strongly than primary tumor growth. This finding suggests that it may be easier to inhibit the neovascularization and growth of a very small tumor and/or micrometastases with a VE-cad antibody, as compared with an established tumor.

Discussion

The results of our studies show that blockade of the VE-cad-mediated homophilic adhesion by systemic administration of the antibody BV13 inhibits angiogenesis, tumor growth, and metastasis. These data demonstrate that VE-cad plays a crucial role in postnatal angiogenesis and validate VE-cad as a potential target for antiangiogenic treatment. Blocking VE-cad represents a novel and unique antiangiogenic mechanism in which the assembly of capillary structures is inhibited. In principle, targeting VE-cad may be generally applied to all angiogenesis settings, regardless of the angiogenic stimulus. VE-cad blockage induces apoptosis in endothelial cells that may be caused by direct apoptotic signaling through phosphatidylinositol 3'-kinase (11) or by the inability of endothelial cells to establish viable connections with their imme-

⁴ F. Liao and E. Dejana, unpublished data.

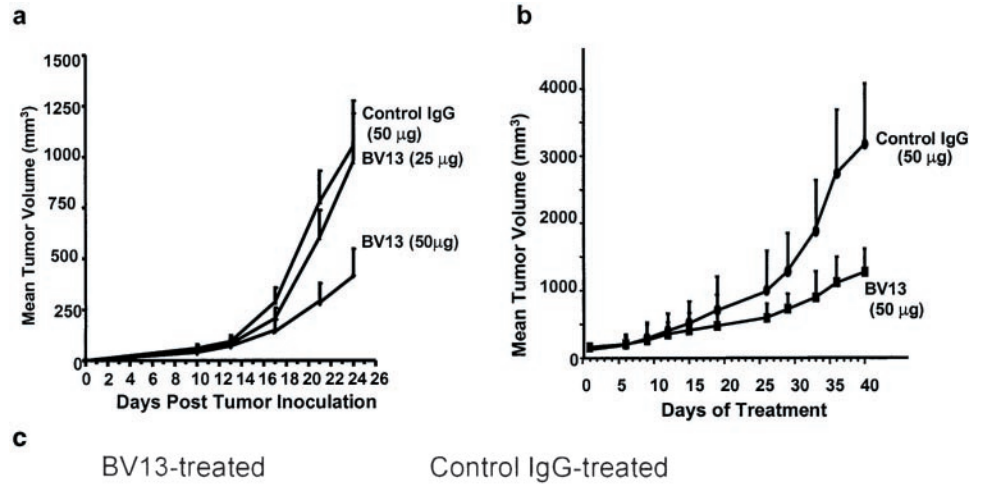


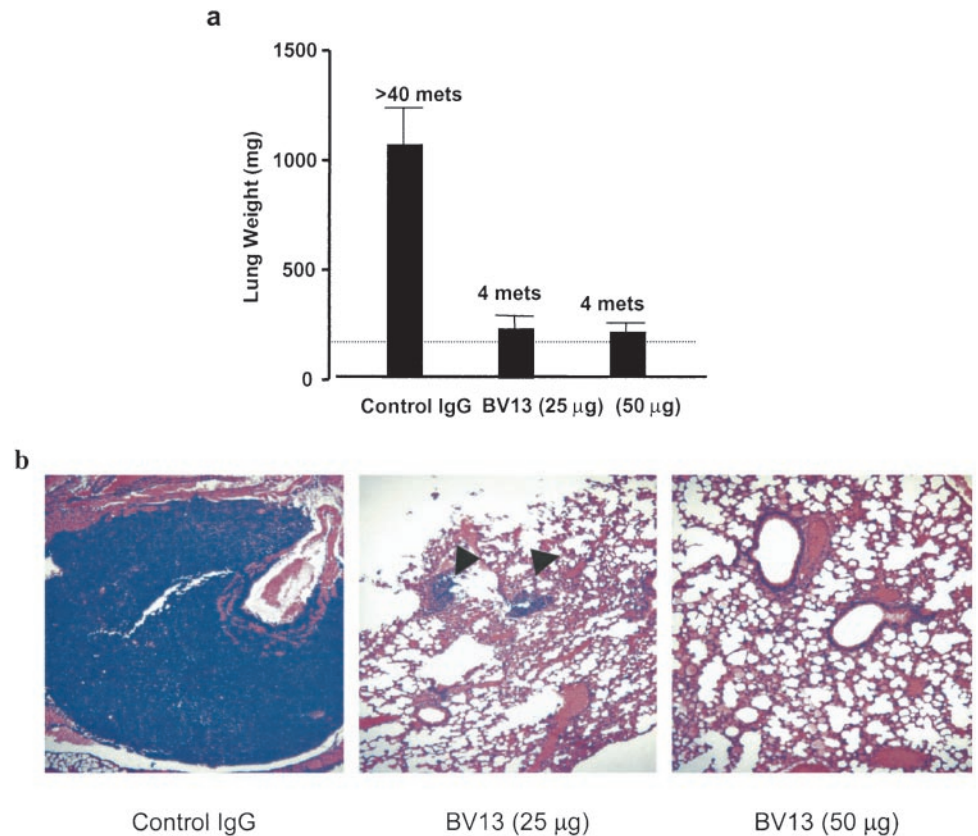
Fig. 3. Effect of antibody BV13 on the growth of s.c. Lewis lung or human A431 epidermoid tumors. *a*, effect of BV13 on the growth of s.c. Lewis lung tumors. Mean \pm SE ($n = 10$) values from a representative experiment are shown. *b*, effect of BV13 on the growth of s.c. A431 human tumor xenografts. Representative data from two experiments are shown as mean tumor volumes \pm SE of 10 mice/group. *c*, histology of 2 week-treated A431 tumor sections. Immunostaining of the paraffin sections for proliferating cell nuclear antigen (brown; $\times 200$) was counterstained with Light Green (Biomed, Foster City, CA). BV13-treated tumor sections show large areas of necrosis and fibrosis. Frozen sections of tumor tissues were examined for PECAM-expressing vessels ($\times 200$) and apoptotic endothelial cells ($\times 400$). A markedly higher frequency of apoptotic endothelial cells was observed in BV13-treated A431 tumors (left panels).

diate environment. Numerous studies have shown that tumor vasculature is uniquely different from that of normal vasculature and is characterized by immature vessels, irregular blood flow, tortuous architecture, and VEGF-induced hyperpermeability (20–23). This study shows that blocking VE-cad with the BV13 antibody further compromises the vasculature in tumors and adds to the growing body of evidence that the structural integrity of tumor blood vessels is unstable in comparison with normal vasculature. The inability to form a functional vasculature in BV13-treated tumors ultimately affected the viability of a dependent tumor mass, as evidenced by massive apoptosis of tumor cells and tumor

necrosis. A similar apoptotic cascade has been induced with other angiogenesis inhibitors acting via entirely different mechanisms, *e.g.*, Flk-1/KDR (19) or $\alpha_v\beta_3$ (24) antagonists.

It is important to note that BV13 has potent *in vivo* antitumor activity at low doses (50 $\mu\text{g}/\text{dose}$). In contrast, other potent antiangiogenic antibodies such as those that block the functions of VEGF (25), VEGF receptor (19), or $\alpha_v\beta_3$ (24) must be given at 10-fold higher doses for comparable effects. Because tumor growth was not completely inhibited by a 50 μg dose of antibody, we attempted to increase dosing to achieve an even better therapeutic result. However, higher doses of BV13 ($>75 \mu\text{g}$, i.p.) resulted in increased vascular

Fig. 4. Effect of antibody BV13 on the growth of Lewis lung metastases. *a*, effect of BV13 on pulmonary metastases of Lewis lung tumor. Data are presented as mean \pm SE of 10 mice/group. Dashed line represents average weight of normal lungs. *b*, H&E staining of lung sections from representative mice in the control group or mice treated with 50 μ g of BV13. Note the large tumor mass found in control lung, whereas only small microscopic nests of tumor cells were observed in lungs from mice treated with 25 μ g of BV13 (arrowheads), and no tumor foci were observed in 7 of 10 mice in the group treated with 50 μ g of BV13.



permeability and edema in the lung followed by the death of some animals within 24–48 h. These findings are similar to our previously reported results (13), where we found that BV13 administered at doses ≥ 50 μ g by i.v. injection resulted in increased vascular permeability, edema in the lungs, and death of some animals. The slight difference in dose and route of administration required to increase lung permeability is likely due to differences in systemic uptake, peak serum levels, and clearance of BV13 when administered by an i.p. versus an i.v. route. Although not performed in these studies, our pharmacokinetic studies with other rat antibodies in mice clearly show a lower maximal antibody serum concentration when systemic administration is via an i.p. route versus an i.v. injection. The permeability effect of BV13 on normal tissues is not entirely unexpected because VE-cad is equally expressed in tumor and normal vasculature.⁵ It should also be noted that BV13 does not preferentially distribute to tumor blood vessels; rather, it can bind to vessels in several tissues (13).⁶ Therefore, anti-VE-cad antibodies may not only prevent the formation of adherens junctions in nascent vasculature (“junction formation”) but may also interfere with established adherens junctions and thus cause increased permeability of the affected vasculature (“junction disruption”). We hypothesize that the VE-cad molecules on the tumor vasculature are more “susceptible” to a therapeutic dose of an antibody due to its poor structural integrity and active angiogenesis. Indeed, we did not observe increased permeability in the lung or other tissues at the therapeutically efficacious dose of 50 μ g, nor did we observe other overt signs of toxicity during the course of treatment in a large number of animals used in a variety of studies.

Our results indicate that antibody BV13 would not be an appropriate agent for therapeutic use due to its disrupting activity on existing adherens junctions. We thus aim at identifying a more desirable

anti-VE-cad angiogenesis inhibitor that would only inhibit adherens junction formation during assembly of vascular tubes but would have a negligible effect on existing junctions of established vessels. Additional studies will determine whether antibodies can be identified that preferentially effect only endothelium undergoing angiogenesis. However, it seems reasonable to anticipate that such antibodies can be developed. VE-cad is a large, transmembrane protein with five extracellular domains that mediate the formation and maintenance of adherens junctions through homophilic interactions. Specific regions of the VE-cad molecule responsible for homophilic interactions and adherens junction formation have not yet been defined. However, assuming that VE-cad-mediated adhesion is as complex as that of other classical cadherins (26, 27), the formation of adherens junctions is likely to involve multiple adhesive contacts between the multiple domains along the extracellular region of VE-cad (28). Thus, it may be possible to target regions of the VE-cad protein that are responsible for one or more steps in the formation of adherens junctions but are not accessible or influenced once adherens junctions have formed. Indeed, in preliminary work using screening assays that distinguish between junction formation and disruption, we have identified unique VE-cad antibodies that inhibit adherens junction formation but do not disrupt existing junctions. Detailed analysis of these antibodies in animal models and of the VE-cad epitopes that give rise to differentially acting antibodies may lead to the identification of antibodies with high therapeutic potential for antiangiogenic treatment.

Acknowledgments

We thank Dawn Dellaratta, Haijun Sun, Marc Rothman, and Karen King for technical support and Drs. L. Eisenbach and T. N. Sato for supplying the D122-96 and bEND.3 cell lines, respectively.

⁵ E. Dejana and A. Hooper, unpublished data.

⁶ E. Dejana, unpublished data.

References

- Hanahan, D., and Folkman, J. Patterns and emerging mechanisms of the angiogenic switch during tumorigenesis. *Cell*, 86: 353–364, 1996.
- Dvorak, H. F., Nagy, J. A., Feng, D., Brown, L. F., and Dvorak, A. M. Vascular permeability factor/vascular endothelial growth factor and the significance of microvascular hyperpermeability in angiogenesis. *Curr. Top. Microbiol. Immunol.*, 237: 97–132, 1999.
- Neufeld, G., Cohen, T., Gengrinovitch, S., and Poltorak, Z. Vascular endothelial growth factor (VEGF) and its receptors. *FASEB J.*, 13: 9–22, 1999.
- Friedlander, M., Brooks, P. C., Shaffer, R. W., Kincaid, C. M., Varner, J. A., and Chesh D. A. Definition of two angiogenic pathways by distinct α , integrins. *Science (Washington DC)*, 270: 1500–1502, 1995.
- Min, H. Y., Doyle, L. V., Vitt, C. R., Zandonella, C. L., Stratton-Thomas, J. R., Shuman, M. A., and Rosenberg, S. Urokinase receptor antagonists inhibit angiogenesis and primary tumor growth in syngeneic mice. *Cancer Res.*, 56: 2428–2433, 1996.
- Drummond, A. H., Beckett, P., Brown, P. D., Bone, E. A., Davidson, A. H., Galloway, W. A., Gearing, A. J., Huxley, P., Laber, D., McCourt, M., Whittaker, M., Wood, L. M., and Wright, A. Preclinical and clinical studies of MMP inhibitors in cancer. *Ann. N. Y. Acad. Sci.*, 878: 228–235, 1999.
- O'Reilly, M. S., Holmgren, L., Shing, Y., Chen, C., Rosenthal, R. A., Moses, M., Lane, W. S., Cao, Y., Sage, E. H., and Folkman, J. Angiostatin: a novel angiogenesis inhibitor that mediates the suppression of metastases by a Lewis lung carcinoma. *Cell*, 79: 315–328, 1994.
- O'Reilly, M. S., Boehm, T., Shing, Y., Fukai, N., Vasios, G., Lane, W. S., Flynn, E., Birkhead, J. R., Olsem, B. R., and Folkman, J. Endostatin: an endogenous inhibitor of angiogenesis and tumor growth. *Cell*, 88: 277–285, 1997.
- Breviario, F., Caveda, L., Corada, M., Martin-Padura, I., Navarro, P., Golay, J., Inrona, M., Gulino, D., Lampugnani, M-G., and Dejana, E. Functional properties of human vascular endothelial cadherin (7B4/cadherin-5), an endothelium-specific cadherin. *Arterioscler. Thromb. Vasc. Biol.*, 15: 1229–1239, 1995.
- Breier, G., Breviario, L., Caveda, L., Berthier, R., Schnurch, H., Gotsch, U., Vestweber, D., Risau, W., and Dejana, E. Molecular cloning and expression of murine vascular endothelial-cadherin in early stage development of cardiovascular system. *Blood*, 87: 630–641, 1996.
- Carmeliet, P., Lampugnani, M. G., Moons, L., Breviario, F., Compernelle, V., Bono, F., Balconi, G., Spagnuolo, R., Oosthuysse, B., Dewerchin, M., Zanetti, A., Angellilo, A., Mattot, V., Nuyens, D., Lutgens, E., Clotman, F., Ruiter, M. A. D., Groot, A. G., Poelmann, R., Lupu, F., Herbert, J. M. Collen, D., and Dejana, E. Targeted deficiency or cytosolic truncation of the VE-cadherin gene in mice impairs VEGF-mediated endothelial survival and angiogenesis. *Cell*, 98: 147–157, 1999.
- Caveda, L., Martin-Padura, I., Navarro, P., Breviario, F., Corada, M., Gulino, D., Lampugnani, M. G., and Dejana, E. Inhibition of cultured cell growth by vascular endothelial cadherin (cadherin-5/VE-cadherin). *J. Clin. Invest.*, 98: 886–893, 1996.
- Corada, M., Mariotti, M., Thurston, G., Smith, K., Kunkel, R., Brockhaus, M., Lampugnani, M. G., Martin-Padura, I., Stoppacciaro, A., Ruco, L., and Dejana, E. VE-cadherin is an important determinant of microvascular integrity *in vivo*. *Proc. Natl. Acad. Sci. USA*, 96: 9815–9820, 1999.
- Bach, T. L., Barsigian, C., Chalupowicz, D. G., Busler, D., Yaen, C. H., Grant, D. S., and Martinez, J. VE-cadherin mediates endothelial cell capillary tube formation in fibrin and collagen gels. *Exp. Cell Res.*, 238: 324–334, 1998.
- Montesano, R., Pepper, M. S., Mohle-Steinlein, U., Risau, W., Wagner, E. F., and Orci, L. Increased proteolytic activity is responsible for the aberrant morphogenetic behavior of endothelial cells expressing the middle T oncogene. *Cell*, 62: 435–445, 1990.
- Dong, Q. G., Bernasconi, S., Lostaglio, S., Decalmanovici, R. W., Martin-Padura, I., Breviario, F., Garlanda, C., Ramponi, S., Mantovari, A., and Vecchi, A. A general strategy for isolation of endothelial cells from murine tissues. Characterization of two endothelial cell lines from the murine lung and subcutaneous sponge implants. *Arterioscler. Thromb. Vasc. Biol.*, 17: 1599–1604, 1997.
- Corada, M., Liao, F., Lindgren, M., Lampugnani, M-G., Breviario, F., Frank, R., Muller, W. A., Hicklin, D. J., Bohlen, P., and Dejana, E. Monoclonals directed to different regions of VE-cadherin extracellular domain may affect adhesion and clustering of the protein and modulate endothelial permeability. *Blood*, in press, 2001.
- Kenyon, B. M., Voest, E. E., Chen, A. A., Flynn, E., Folkman, J., and D'Amato, R. J. A model of angiogenesis in the mouse cornea. *Invest. Ophthalmol. Visual Sci.*, 37: 1625–1632, 1996.
- Prewett, M., Huber, J., Li, Y., Santiago, A., O'Connor, W., King, K., Overholser, J., Hooper, A., Pytowski, B., Witte, L., Bohlen, P., and Hicklin D. J. Antivascular endothelial growth factor receptor (fetal liver kinase 1) monoclonal antibody inhibits tumor angiogenesis and growth of several mouse and human tumors. *Cancer Res.*, 59: 5209–5218, 1999.
- Roberts, W. G., and Palade, G. E. Neovasculature induced by vascular endothelial growth factor is fenestrated. *Cancer Res.*, 57: 765–772, 1997.
- Benjamin, L. E., Golijanin, D., Itin, A., Pode, D., and Keshet, E. Selective ablation of immature blood vessels in established human tumors follows vascular endothelial growth factor withdrawal. *J. Clin. Invest.*, 103: 159–165, 1999.
- Dvorak, H. K., Brown, L. F., Detmar, M., and Dvorak, A. M. Vascular permeability factor/vascular endothelial growth factor, microvascular hyperpermeability, and angiogenesis. *Am. J. Pathol.*, 146: 1029–1039, 1995.
- Jain, R. K. Determinants of tumor blood flow: a review. *Cancer Res.*, 48: 2641–2658, 1988.
- Brooks, P. C., Montgomery, A. M. P., Rosenfeld, M., Reisfeld, R. A., Hu, T., Klier, G., and Chesh, D. A. Integrin $\alpha_v\beta_3$ antagonists promote tumor regression by inducing apoptosis of angiogenic blood vessels. *Cell*, 79: 1157–1164, 1994.
- Kim, J., Li, B., Winer, J., Armenini, M., Gillett, N., Phillip, H. S., and Ferrara, N. Inhibition of vascular endothelial growth factor-induced angiogenesis suppresses tumor growth *in vivo*. *Nature (Lond.)*, 362: 841–844, 1993.
- Nollet, F., Kools, P., and Roy, F. Phylogenetic analysis of the cadherin superfamily allows identification of six major superfamilies besides several solitary members. *J. Mol. Biol.*, 299: 551–572, 2000.
- Yagi, T., and Takeichi, M. Cadherin superfamily genes: functions, genomic organization, and neurologic diversity. *Genes Dev.*, 14: 1169–1180, 2000.
- Sivasankar, S., Brieher, W., Lavrik, N., Gumbiner, B., and Leckband, D. Direct molecular force measurements of multiple adhesive interactions between cadherin ectodomains. *Proc. Natl. Acad. Sci. USA*, 96: 11820–11824, 1999.